Journal of Physics: Conference Series **596** (2015) 012001 doi:10.1088/1742-6596/596/1/012001

Dye-sensitized solar cells using double-oxide electrodes: a brief review

Yoshikazu Suzuki,[1,2] Yuji Okamoto[2] and Natsumi Ishii[2]

[1]Faculty of Pure and Applied Sciences, University of Tsukuba, 1-1-1 Tennodai, Tsukuba, Ibaraki, 305-8573, Japan.
[2]Graduate School of Pure and Applied Sciences, University of Tsukuba, 1-1-1 Tennodai, Tsukuba, Ibaraki, 305-8573, Japan.

E-mail: suzuki@ims.tsukuba.ac.jp

Abstract. Dye-sensitized solar cells (DSC or DSSC) have been widely investigated because of their potentially high cost performance compared with Si-based solar cells and of their fascinating appearance. DSC with photoelectric conversion efficiency of >10 % (or even 12 %) have been reported, where porous TiO_2 films are generally used as semi-conductor electrodes. Such porous TiO_2 films usually have high specific surface area, and thus, they adsorb plenty of dye molecules, resulting in high photocurrent density. Recently, some double oxides have been examined as alternative photoanode materials, mainly in order to improve photovoltage. Here, studies on DSC using double-oxide electrodes, i.e., perovskite, spinel, ilmenite, wolframite, scheelite and pseudobrookite-types, are briefly reviewed.

1. Introduction

After the pioneer work on dye-sensitized solar cells (DSC or DSSC) by O'Regan and Grätzel in 1991 [1], wide variety of oxide-based semiconductors, instead of TiO_2, have been studied as alternative electrode materials of DSC. Here, studies on DSC using double-oxide electrodes are briefly reviewed with focusing on the simple replacement for TiO_2, *i.e.*, double-oxide-based phase-pure porous electrode (type A in Fig. 1 [2]) .

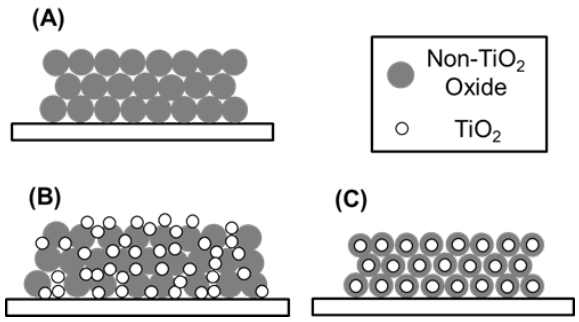

Figure 1. Non-TiO_2 oxides used for DSC electrodes: (A) phase-pure porous electrode, (B) composite electrode with TiO_2, and (C) coating materials on TiO_2. Reproduced with permission from ref. [2] Copyright 2014 The Ceramic Society of Japan.

2. Perovskite-type oxides (ABO_3)

Among various double oxides, perovskite-type oxides have been most widely studied due to the band-structure similarity to TiO_2 anatase. In 1999, Burnside et al. [3] synthesized nanocrystalline mesoporous $SrTiO_3$ by hydrothermal treatment of nanocrystalline TiO_2 and $Sr(OH)_2$ at 190°C for 4.5 h, and applied the obtained nanocrystalline $SrTiO_3$ to photoanodes of DSC by sintering at 500-600°C in a flowing oxygen atmosphere. They confirmed that the dye uptake of the $SrTiO_3$ films was about half of the TiO_2 anatase film, which suggests that the surface treatment of $SrTiO_3$ or the optimization of dye may improve the cell performance.

In 2001, Lenzmann et al. [4] reported $SrTiO_3$ nanocrystalline photoanode, which was evaluated by surface photovoltage spectroscopy. They found a blue shift for the $SrTiO_3$-based cell as compared to the TiO_2 anatase based cell. In 2010, Yang et al. [5] determined the flat band edges (E_{fb}) of nanostructured $SrTiO_3$ electrodes in propionitrile (PN), acetylacetone (Acac) and PN/Acac mixture. They also prepared N3-dye sensitized $SrTiO_3$ and evaluated its photovoltage-photocurrent curves (Table 1). They reported short-circuit current density (J_{SC}), open-circuit voltage (V_{OC}) and *I-V* curves of N3-dye sensitized $SrTiO_3$, but the power conversion efficiency (PCE) was not stated in detail.

In 2014 (online in Oct. 2013), based on the Yang's work [5], Jayabal et al. [6] pointed out that (1) both TiO_2 and $SrTiO_3$ have similar band gap of value of ~3.2 eV, but the flat-band potential of $SrTiO_3$ is greater than that of TiO_2 anatase, and (2) the conduction band of $SrTiO_3$ lie ~0.2 eV above the conduction band of TiO_2 anatase, hence $SrTiO_3$ is expected to produce excellent photovoltage. To demonstrate the feasibility of $SrTiO_3$, Jayabal et al. synthesized mesoporous $SrTiO_3$ via hydrothermal treatment of $Sr(CH_3COO)_2$ and $Ti[OCH(CH_3)_2]_4$ at 120°C for 12 h with post calcination at 900°C for 6 h, and they applied it to DSC (Table 1). High V_{OC} of 0.73 eV is ascribed to the more negative positioned conduction band of $SrTiO_3$, and low current density is attributed to the reverse saturation current.

Also in 2014, Okamoto et al. [2] reported the synthesis of $SrTiO_3$, $CaTiO_3$ and $BaTiO_3$ submicron powders by solid-state reaction at 1200°C for 2 h followed by planetary ball-milling, and they applied the powders to DSC (Table 1). Without the optimization of redox electrolyte etc., PCE values of this research were much lower than other works. Still, they succeeded to demonstrate the difference among three perovskite-type electrodes. Note that the $SrTiO_3$ and $BaTiO_3$ powders were effective as second phases of composite type electrodes (type-B in Fig. 1). In 2015 (online in Oct. 2014), Li et al. [7] synthesized Ho^{3+}-doped $SrTiO_3$ in order to obtain the down-conversion effect and p-type doping effect. Although PCE values of their study were also much lower than other works, apparent increase in J_{SC} was confirmed. Besides titanates, other perovskite-type oxides have been also studied, such as barium stannate ($BaSnO_3$) with band gap of 3.1 eV[8,9]. Shin et al. reported the PCE of 4.5% for bare $BaSnO_3$.

Table 1. DSC using perovskite-type double oxide electrodes.

Electrode	Electrode area (cm^2)	Electrode thickness (μm)	Type of dye	Light source (mW/cm^2)	V_{OC} (V)	J_{SC} (mA/cm^2)	FF	PCE η (%)	References
$SrTiO_3$	–	5-6	N3	~100	0.789	3	0.70	1.8	Burnside (1999) [3]
$SrTiO_3$	0.196	–	N3	100	0.6	0.41	–	–	Yang (2010) [5]
$SrTiO_3$	1	–	EY*	62.5	0.73	0.44	0.55	0.51(?)	Jayabal (2014) [6]
$SrTiO_3$	1	~ 10	N719	100	0.636	0.128	0.464	0.038	Okamoto (2014) [2]
$CaTiO_3$	1	~ 10	N719	100	0.488	0.0172	0.312	0.0026	Okamoto (2014) [2]
$BaTiO_3$	1	~ 10	N719	100	0.650	0.127	0.433	0.036	Okamoto (2014) [2]
$SrTiO_3$	0.25	–	N719	100	0.54	0.15	0.51	0.04	Li (2015) [7]
Ho^{3+}-doped $SrTiO_3$	0.25	–	N719	100	0.60	0.23	0.49	0.07	Li (2015) [7]
$BaSnO_3$ (CP)	0.4	~ 10	N719	100	0.68	2.77	0.60	1.1	Guo (2010) [8]
$BaSnO_3$ (HT)	0.4	~ 10	N719	100	0.67	2.04	0.59	0.8	Guo (2010) [8]
$BaSnO_3$ (SSR)	0.4	~ 10	N719	100	0.58	0.37	0.47	0.1	Guo (2010) [8]
$BaSnO_3$	0.16	–	N719	100	0.61	11.19	0.66	4.5	Shin (2013) [9]

*EY: Eosin Yellow, CP: coprecipitation, HT: hydrothermal, SSR: solid-state reaction.

Table 2. DSC using spinel, ilmenite, wolframite, scheelite and pseudobrookite-type double oxide electrodes.

Electrode	Electrode area (cm^2)	Electrode thickness (μm)	Type of dye	Light source (mW/cm^2)	V_{OC} (V)	J_{SC} (mA/cm^2)	FF	PCE η (%)	References
Spinel									
Zn_2SnO_4	0.20	5.6	N719	~100	~0.62	~9.1	~0.67	3.8	Tan (2007) [10]
Zn_2SnO_4	0.32	5.7	N719	100	0.68	2.4	0.68	1.0	Lana-Villarreal (2007) [11]
Mg_2TiO_4	1.0	30.8	N719	100	0.586	0.033	0.293	0.0056	Ishii (2015) [12]
Ilmenite									
$CdSnO_3$	0.2	15	N719	~100	0.43	7.43	0.45	1.42	Natu (2010) [13]
$MgTiO_3$	1.0	28.8	N719	100	0.515	0.048	0.317	0.0079	Ishii (2015) [12]
Wolframite									
$ZnWO_4$	0.25*	~12*	N3*	100	0.57	0.21	0.459	0.054	Kim (2011) [14]
$MgWO_4$	0.25*	~12*	N3*	100	0.46	0.18	0.429	0.036	Kim (2011) [14]
Scheelite									
$CaWO_4$	0.25*	~12*	N3*	100	0.41	0.13	0.422	0.023	Kim (2011) [14]
$SrWO_4$	0.25*	~12*	N3*	100	0.39	0.12	0.433	0.020	Kim (2011) [14]
Pseudobrookite									
$MgTi_2O_5$	1.0	42	N719	100	0.465	0.060	0.248	0.0069	Ishii (2015) [12]

*Jung et al. [15]

3. Spinel-type oxides (AB_2O_4)

Spinel-type double oxide group (general formula: AB_2O_4) also contains many compounds. Some spinel-type oxides have been examined as photoanodes of DSC. In 2007, Tan et al. [10] examined zinc stannate, Zn_2SnO_4 (inverse spinel type, $Zn[Zn,Sn]O_4$) with band gap of 3.6 eV, and reported the PCE of 3.8%. According to Tan et al., the electron diffusion length for Zn_2SnO_4 is shorter than P25 TiO_2 film. However, for thin films (≤ ~ 6 μm), the photocurrent density for a Zn_2SnO_4 cell was higher than that for a P25 cell with the same film thickness. Lana-Villarreal et al. [11] also reported the DSC performance of Zn_2SnO_4 DSC.

In 2015, Ishii et al. [12] reported Mg_2TiO_4 (inverse spinel type) with band gap of 3.7 eV as a photoanode of DSC. In their preliminary data, since Mg_2TiO_4 particles were large and film thickness was not optimized (too thick as a photoelectrode), DSC performance was rather low. Similar to Zn_2SnO_4, the electron diffusion length for Mg_2TiO_4 may be shorter than TiO_2. Further optimization will be expected.

4. Ilmenite-type oxides (ABO_3)

When the ionic radii of A and B ions in ABO_3 are similar to each other, ilmenite-type double oxides preferably form instead of perovskite-type. Some ilmenite-type oxides also have been studied as photoanodes of DSC. In 2010, Natu and Wu [13] studied cadmium stannate, $CdSnO_3$ with band gap of 3.07 eV, and reported the PCE of 1.42%. The conduction band edge of $CdSnO_3$ is ca. 0.9 eV lower than that of TiO_2 anatase. A merit of $CdSnO_3$ double oxide is its higher stability in an acidic environment than SnO_2. Ishii et al. [12] also preliminary reported on $MgTiO_3$ with band gap of 3.7 eV as a photoanode of DSC.

5. Wolfamite and scheelite-type oxides (MWO_4)

In 2011, Kim et al. [14,15] prepared divalent metal tungstates, MWO_4, with wolframite (M=Zn and Mg) and scheelite (M=Ca and Sr) structures by a solid-state reaction method, and applied them for DSC. Wolframite-type showed better performance than scheelite-type, which is attributable to their enhanced electron transfer resulting from appropriate band positions. The band gaps of $ZnWO_4$, $MgWO_4$, $CaWO_4$ and $SrWO_4$ are 2.95, 3.48, 4.25 and 4.58 eV, respectively. Correspondingly, the PCE of $ZnWO_4$, $MgWO_4$, $CaWO_4$ and $SrWO_4$ were 0.054, 0.036, 0.023 and 0.020%, respectively.

6. Pseudobrookite-type oxides (M_3O_5)

Another double oxide in MgO-TiO_2 binary system, $MgTi_2O_5$ (pseudobrookite, band gap of 3.4 eV) was also preliminary studied by Ishii et al. [12].

7. Conclusion

Studies on DSC using perovskite, spinel, ilmenite, wolframite, scheelite and pseudobrookite-type double oxides are briefly reviewed. Common positive aspect using double oxide will be their flexibility of band tuning. Perovskite-type $BaSnO_3$ and spinel-type Zn_2SnO_4 are most promising to date. Compared with conventional TiO_2-based DSC, however, further optimization is required.

Acknowledgment

This work was supported by Grant-in-Aid for Science Research No. 23350111 (Basic Research: Category B), University of Tsukuba-NIMS Collaborative Research Project, and JST/ACT-C "Creation of methanol synthesis catalysts working at room temperature based on mechanistic principles of CO_2 activation" head by Prof. Junji Nakamura.

References

[1] O'Regan B and Grätzel M 1991 *Nature* **353** 737.
[2] Okamoto Y and Suzuki Y 2014 *J. Ceram. Soc. Jpn*. **122** 728.
[3] Burnside S, Moser J E, Brooks K, Grätzel M and Cahen D, 1999 *J. Phys. Chem. B* **103** 9328.
[4] Lenzmann F, Krueger J, Burnside S, Brooks K, Grätzel M, Gal D, Ruhle S and Cahen D 2001 *J. Phys. Chem. B* **105** 6347.
[5] Yang S M, Kou H, Wang J C, Xue H B and Han H L 2010 *J. Phys. Chem. C* **114** 4245.
[6] Jayabal P, Sasirekha V, Mayandi J, Jeganathan K and Ramakrishnan V 2014 *J. Alloy Compd*. **586** 456.
[7] Li Y Y, Hao H S, Qin L, Wang H L, Nie M Q, Hu Z Q, Gao W Y and Liu G S 2015 *J. Alloy Compd*. **622** 1.
[8] Guo F A, Li G Q and Zhang W F 2010 *Int. J. Photoenergy* **2010** 105878.
[9] Shin S S, Kim J S, Suk J H, Lee K D, Kim D W, Park J H, Cho I S, Hong K S and Kim J Y 2013 *ACS Nano* **7** 1027.
[10] Tan B, Toman E, Li Y G and Wu Y Y 2007 *J. Am. Chem. Soc.* **129** 4162.
[11] Lana-Villarreal T, Boschloo G and Hagfeldt A 2007 *J. Phys. Chem. C* **111** 5549.
[12] Ishii N, Okamoto Y and Suzuki Y 2015 *Int. Lett. Chem. Phys. Astro*. **7** 9.
[13] Natu G and Wu Y Y 2010 *J. Phys. Chem. C* **114** 6802.
[14] Kim D W, Cho I S, Shin S S, Lee S, Noh T H, Kim D H, Jung H S and Hong K S 2011 *J. Solid State Chem.* **184** 2103.
[15] Jung H S, Lee J K, Lee S, Hong K S and Shin H 2008 *J. Phys. Chem. C* **112** 8476.